

## Resonant transfer and excitation in ion-atom collisions

D. Brandt

*Department of Physics and Astronomy, University of North Carolina,  
Chapel Hill, North Carolina 27514*

(Received 13 July 1982)

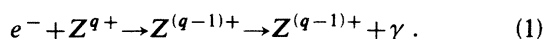
In the resonant (charge) transfer and excitation (RTE) process, resonance states in the charge-changed projectile are formed due to Coulomb interaction with the target electrons. The calculated RTE cross section is proportional to the cross section for dielectronic recombination and its projectile energy dependence reflects the momentum distribution of the target electrons. Sample calculations for  $K$  x-ray production in  $\text{Si}^{11+} + \text{He}$ ,  $\text{S}^{13+} + \text{Ar}$ , and  $\text{S}^{13+} + \text{He}$  collisions are discussed. An estimate of the experimental background indicates that RTE is more pronounced in collisions with light targets.

## I. INTRODUCTION

In a fast collision of a highly charged ion with a target atom, projectile vacancy production is mostly due to Coulomb interaction with the target nucleus.<sup>1</sup> It has recently been recognized,<sup>2-4</sup> however, that for certain collision energies the interaction of a target electron with the projectile may give a significant contribution to the excitation of a particular projectile state. This resonant transfer and excitation (RTE) process will occur if a target electron is captured into a resonance state of the projectile.

## II. DESCRIPTION OF RTE

In order to describe RTE, it is useful first to consider radiationless capture (RC) and dielectronic recombination (DR)<sup>5,6</sup> in electron-ion collisions,



Here, a free electron with the momentum  $p$ , mass  $m$ , and the kinetic energy

$$\epsilon = p^2/2m \quad (2)$$

collides with a positive ion of charge state  $q$  and is captured into an intermediate resonance state (RC). This resonance state will subsequently decay either by Auger electron emission or by photon emission (DR). In the isolated resonance approximation the DR cross section<sup>7</sup>

$$\sigma_{\text{DR}} \sim w/p^2 V(i \rightarrow r) \Gamma [(\epsilon - \epsilon_\mu)^2 + \Gamma^2/4]^{-1} \quad (3)$$

is given by the product of the RC cross section  $\sigma_{\text{RC}}$  and the fluorescence yield  $w$  for the particular resonance state

$$\sigma_{\text{DR}} = w \sigma_{\text{RC}}. \quad (4)$$

Here,  $V(i \rightarrow r)$  is the excitation-capture probability, and  $\Gamma$  is the width of the resonance. RC and DR are resonant processes which will only take place if the energy  $\epsilon$  of the electron in the rest frame of the ion matches the energy difference  $\epsilon_r$  of the resonance and initial ion states, i.e., the corresponding Auger energy.

McLaughlin and Hahn<sup>7</sup> have calculated DR cross sections for several resonance states of  $\text{Si}^{10+}$  and  $\text{S}^{12+}$ , which will be used for sample calculations of RTE cross sections later on. They present their results in a form

$$\bar{\sigma}_{\text{DR}} = 1/\Delta\epsilon \int_{\epsilon_r - \Delta\epsilon/2}^{\epsilon_r + \Delta\epsilon/2} d\epsilon \sigma_{\text{DR}}(\epsilon) = w \bar{\sigma}_{\text{RC}}, \quad (5)$$

where the cross section is averaged over a bin  $\Delta\epsilon = 1$  Ry of electron energies centered around  $\epsilon_r$ . It should be noted that  $\Delta\epsilon \bar{\sigma}_{\text{DR}}$  is constant as long as  $\Delta\epsilon$  is large compared to the width of the resonance  $\Gamma$ .

In RTE, the projectile ion captures not a free electron as in RC but a bound target electron. Under conditions which allow neglect of the dynamic aspects of the interaction between the electrons and the target nucleus (impulse approximation, see Sec. III), the target electron may be characterized by its momentum distribution. Thus in the rest frame of the projectile, the target electron populates a continuous distribution of energies. In this respect RTE bears much similarity to radiative electron capture (REC)<sup>8-10</sup> of a bound target electron into an inner shell of the projectile. The difference is, however, that in REC the electron can be captured from a continuum state of any energy into a bound state of the projectile, the excess energy being taken away by photon emission (inverse of the photoelectric effect), whereas in RTE the energy of the initial continuum state has to match the energy of the intermediate

resonance state (inverse of the Auger effect). It is interesting to note that in the limit of very low collision velocities, REC and RTE correspond to molecular orbital (MO) x-ray emission<sup>9-11</sup> and molecular autoionization,<sup>12,13</sup> respectively.

### III. IMPULSE APPROXIMATION

In the following, the impulse approximation<sup>14</sup> is applied to relate the RTE cross section to the RC cross section for a free electron. This is directly analogous to the calculation by Kleber and Jakubassa,<sup>9</sup> in which the cross section for REC is related to the cross section for radiative capture of a free electron. It is assumed that the collision velocity is large compared to the velocity of the target electrons and that the distortion of the projectile resonance state by the target nucleus is small.

If  $\vec{p}_i$  is the electron momentum of a specific target electron in the target frame, then the momentum of this electron in the projectile rest frame is given by

$$\vec{p} = \vec{p}_0 + \vec{p}_i, \quad (6)$$

where

$$p_0 = m(2E/M)^{1/2} \quad (7)$$

is the average momentum of the electron with respect to the projectile,  $E$  is the laboratory projectile energy, and  $M$  is the mass of the projectile.

In the impulse approximation the cross section  $\sigma_{RC}$  for the production of a particular resonance state in ion-electron collisions and the cross section  $\sigma_{RTE}$  for the production of the same resonance state in ion-atom collisions are related by

$$\sigma_{RTE} = \int_{-\infty}^{+\infty} d^3\vec{p}_i (\sigma_{RC})_p |\psi_i(\vec{p}_i)|^2. \quad (8)$$

The momentum wave function  $\psi_i(\vec{p}_i)$  of the target electron is assumed to be undisturbed, and  $(\sigma_{RC})_p$  is the RC cross section for a free electron of momentum  $p$  with respect to the ion

$$p = (p_0^2 + p_i^2 + 2p_0 p_{iz})^{1/2}. \quad (9)$$

The projectile energy dependence of  $\sigma_{RTE}$  enters through the dependence of  $p$  on  $p_0$ . For small electron momenta,

$$p_i \ll p_0, \quad (10)$$

the quadratic term in  $p_i$  can be neglected,

$$p \approx (p_0^2 + 2p_0 p_{iz})^{1/2}. \quad (11)$$

Then, the RC cross section depends only on the component  $p_{iz}$  of  $\vec{p}_i$  parallel to  $\vec{p}_0$ ,

$$\sigma_{RTE} = \int_{-\infty}^{+\infty} dp_{iz} \sigma_{RC}(p_{iz}) \times \int \int dp_{ix} dp_{iy} |\psi_i(\vec{p}_i)|^2. \quad (12)$$

Introducing the Compton profile  $J_i(p_{iz})$ ,

$$J_i(p_{iz}) = \int \int_{-\infty}^{+\infty} dp_{ix} dp_{iy} |\psi_i(\vec{p}_i)|^2, \quad (13)$$

which gives the probability of finding a particular target electron with a momentum component  $p_{iz}$ ; it follows that

$$\sigma_{RTE} = \int_{-\infty}^{+\infty} dp_{iz} \sigma_{RC}(p_{iz}) J_i(p_{iz}). \quad (14)$$

The RC cross section is sharply peaked around  $p = p_r$ ,

$$p_r = (2m\epsilon_r)^{1/2}. \quad (15)$$

Hence it contributes to the integral (14) only for values  $p_{iz}$  close to  $p_{iz} = p'_r$ ,

$$p'_r = (\epsilon_r - Em/M)(M/2E)^{1/2}. \quad (16)$$

The Compton profile, on the other hand, varies comparatively slowly as a function of  $p_{iz}$ , so that it may be taken out of the integral,

$$\sigma_{RTE} = J_i(p'_r) \int_{-\infty}^{+\infty} dp_{iz} \sigma_{RC}(p_{iz}). \quad (17)$$

The reasonableness of this approximation may be illustrated by a typical example for the width of  $\sigma_{RC}(p_{iz})$  and  $J_i(p_{iz})$ . Assuming a resonance width  $\Gamma = 0.02$  a.u. and a projectile momentum  $p_0 = 10$  a.u., the width of  $\sigma_{RC}(p_{iz})$  comes out to be about 0.002 a.u. [full width at half maximum (FWHM)]. This may be compared to a value of about 1.6 a.u. for the width of the He Compton profile (FWHM).

Replacing the integration variable  $p_{iz}$  by the kinetic energy  $\epsilon$  of the electron in the projectile frame

$$\epsilon = Em/M + p_{iz}(2E/M)^{1/2} \quad (18)$$

and restricting the integration to a finite range  $\Delta\epsilon > \Gamma$  around  $\epsilon = \epsilon_r$ , it follows that

$$\sigma_{RTE} = (M/2E)^{1/2} J_i(p'_r) \times \int_{\epsilon_r - \Delta\epsilon/2}^{\epsilon_r + \Delta\epsilon/2} d\epsilon \sigma_{RC}(\epsilon). \quad (19)$$

The integral in Eq. (19) is proportional to the energy averaged cross section for RC [see Eq. (5)],

$$\sigma_{RTE} = (M/2E)^{1/2} \Delta\epsilon \bar{\sigma}_{RC} J_i(p'_r). \quad (20)$$

The projectile energy dependence of  $\sigma_{RTE}$  is mostly determined by the implicit dependence (16) of  $J_i(p'_r)$  on  $E$ . It exhibits a maximum close to  $E = E_{\max}$ ,

$$E_{\max} = \epsilon_r M/m, \quad (21)$$

since the Compton profile has its maximum at

$p_{iz}=0$ .

The RTE cross section for a certain target atom is derived by summing over the contributions of all target electrons, denoted by the subscript  $i$ ,

$$\sigma_{\text{RTE}}(\text{tot})=(M/2E)^{1/2}\Delta\epsilon\bar{\sigma}_{\text{RC}}\sum J_i(p'_{iz}). \quad (22)$$

The cross section  $\sigma_{\text{RTE}}^{\text{Au}}$  for RTE followed by Auger electron emission is then

$$\sigma_{\text{RTE}}^{\text{Au}}=(1-w)\sigma_{\text{RTE}} \quad (23)$$

and the cross section  $\sigma_{\text{RTE}}^{\text{x}}$  for RTE followed by x-ray emission is given by

$$\sigma_{\text{RTE}}^{\text{x}}=(M/2E)^{1/2}\Delta\epsilon\bar{\sigma}_{\text{DR}}\sum J_i(p'_{iz}). \quad (24)$$

This can be compared directly with calculations of DR cross sections, which implicitly include the fluorescence yield  $w$ .<sup>7</sup>

It should be noted that the above calculations rely on the validity of condition (10), which is fulfilled best for projectile energies close to  $E_{\text{max}}$  [compare Eqs. (16) and (21)] and electrons with a small average momentum

$$|\bar{p}_i| < p_r, \quad (25)$$

i.e., for light target atoms with narrow electron momentum distributions and for heavy projectiles with high Auger energies.

In conclusion, the RTE cross section is found to be proportional to the energy averaged DR cross section and a sum over the Compton profiles of the target electrons. Varying the projectile energy  $E$  has the effect of scanning the Compton profiles of the target electrons, so that  $\sigma_{\text{RTE}}$  reflects the momentum distribution of the target electrons in much the same way as the REC cross section as a function of the photon energy does.

#### IV. DISCUSSION OF SAMPLE CALCULATIONS

Figure 1 shows calculated RTE x-ray cross sections as a function of projectile energy from the decay of the resonance states  $\text{Si}^{10+} 1s 2s 2p^2 S + D$  and  $\text{S}^{12+} 1s 2s 2p^2 S + D$  in  $\text{Si}^{11+} + \text{He}$  and  $\text{S}^{13+} + \text{Ar}$  collisions, respectively. McLaughlin and Hahn<sup>7</sup> calculated these to be the most prominent  $K$  excited resonance states with Auger energies and energy-averaged DR cross sections ( $\Delta\epsilon=1$  Ry) of  $\epsilon_r=1427$  eV,  $\bar{\sigma}_{\text{DR}}=1.89\times 10^{-20}$  cm<sup>2</sup> for  $\text{Si}^{10+}$  and  $\epsilon_r=1850$  eV and  $\bar{\sigma}_{\text{DR}}=2.40\times 10^{-20}$  cm<sup>2</sup> for  $\text{S}^{12+}$ . The Compton profiles for the He and Ar target electrons are taken from tabulated Hartree-Fock calculations.<sup>15</sup>

For the  $\text{Si}^{11+} + \text{He}$  collisions the cross-section maximum occurs at 72-MeV projectile energy, close

to  $E_{\text{max}}=73$  MeV, as expected from Eq. (21). The shape of the RTE peak shows an asymmetry, even though the Compton profile  $J(p_{iz})$  is symmetric with respect to  $p_{iz}=0$ . This asymmetry is mainly due to the nonlinear relation (16) between  $p'_{iz}$  and  $E$ .

The RTE cross section calculation for  $\text{S}^{13+} + \text{Ar}$  collisions corresponds to the experiment reported by Tanis *et al.*<sup>2,4</sup> Here, target electrons from different shells contribute to the cross section. The Ar  $M$  electrons contribute the most to the calculated maximum at 106-MeV projectile energy due to their narrow Compton profiles. The Ar  $1s$  electrons are not included in the calculation, because their inner velocity exceeds the projectile velocity and thus they do not qualify for the impulse approximation; their contribution to the yield of the observed process is expected to be small. For the  $\text{S}^{13+} + \text{Ar}$  collision system the RTE peak is broader than for the  $\text{Si}^{11+} + \text{He}$  collision system, due to the following two reasons: The RTE feature can be viewed as a magnified image of the respective Compton profiles, the magnification and thus the width increasing with  $E_{\text{max}}$ ; the other reason is that the total Ar Compton profile constructed from the Compton profiles for the Ar  $L$  and  $M$  electrons is broader than the total He Compton Profile. This also causes the ratio of the  $\text{S}^{13+} + \text{Ar}$  and  $\text{Si}^{11+} + \text{He}$  RTE cross-section maxima to be only  $\approx 5$ , even though the ratio of the number of target electrons participating in the two cases is 8, and the respective DR cross sections are equal within 25%.

For a quantitative comparison with the  $\text{S}^{13+} + \text{Ar}$  experiment<sup>4</sup> the contributions of all resonance states

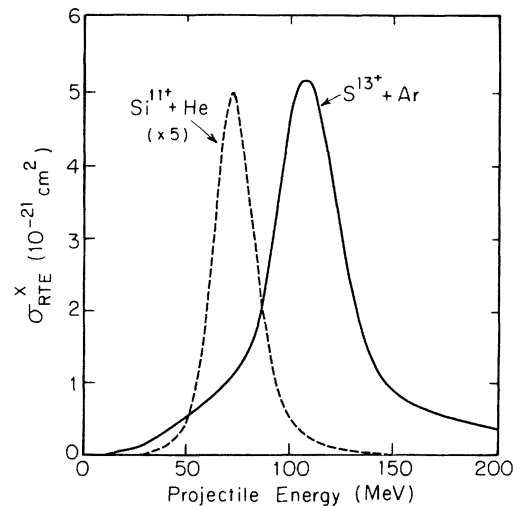


FIG. 1. RTE x-ray production cross section from the decay of the  $\text{S}^{12+} 1s 2s 2p^2 S + D$  states in  $\text{S}^{13+} + \text{Ar}$  collisions (solid line) and from the decay of the  $\text{Si}^{10+} 1s 2s 2p^2 S + D$  states in  $\text{Si}^{11+} + \text{He}$  collisions (dashed line).

as calculated by McLaughlin and Hahn<sup>7</sup> have been added up, since the corresponding x-ray energies are not resolved experimentally. The resulting x-ray cross section is shown in Fig. 2. It has a maximum value of  $1.23 \times 10^{-20}$  cm<sup>2</sup> at 120-MeV projectile energy and a FWHM of 61 MeV. The calculation includes resonance states with energies  $\epsilon_r$ , ranging from 1817.6 eV for the  $S^{12+} 1s 2s^2 2p^1 P$  state to the series limit at 2421.7 eV. These correspond to RTE cross-section maxima for the individual states at projectile energies between 105 and 140 MeV. They are not resolved, however, since the RTE peaks for each state are quite broad because of the width of the Ar Compton profile. Also shown in Fig. 2 is a calculation for the collision system  $S^{13+} + He$ . Here, some structure in the RTE cross section can be observed, since the He Compton profile is narrower than the Ar Compton profile. The cross-section maximum of  $2.25 \times 10^{-21}$  cm<sup>2</sup> occurs at 125 MeV in this case, and the FWHM is 54 MeV.

The signature of RTE is that the cross section for the formation of a particular resonance state in the charge-changed projectile depends in a characteristic way on the energy of the incident ion. The decay of this state can then be monitored by detecting characteristic x rays and/or Auger electrons in high resolution.

There is, however, a competing process for the formation of resonance states due to projectile excitation by the target nucleus and one-electron capture in the same collision. If the probability for excitation  $P_{ex}(b)$  and the probability for capture  $P_{cap}(b)$  are uncorrelated, the integration over all impact parameters  $b$  yields

$$\sigma_{ex\,cap} = 2\pi \int_0^\infty P_{ex}(b)P_{cap}(b)b\,db \quad (26)$$

for the cross section  $\sigma_{ex\,cap}$  of the competing process. The magnitude and the projectile energy dependence of  $\sigma_{ex\,cap}$  will vary for different collision systems. A qualitative feature concerning the target nuclear charge  $Z_T$  should be mentioned though.

With increasing  $Z_T$  the probability for projectile excitation due to Coulomb interaction with the target nucleus becomes larger and so does the capture probability since more target electrons are available for capture. As the main contribution for  $\sigma_{RTE}$  stems only from the outer target electrons, the ratio  $\sigma_{RTE}/\sigma_{ex\,cap}$  is likely to decrease with increasing  $Z_T$ , even if the absolute magnitude of  $\sigma_{RTE}$  increases (see Fig. 2).

## V. CONCLUSION

RTE contributes in a characteristic way to the projectile vacancy production in ion-atom collisions.

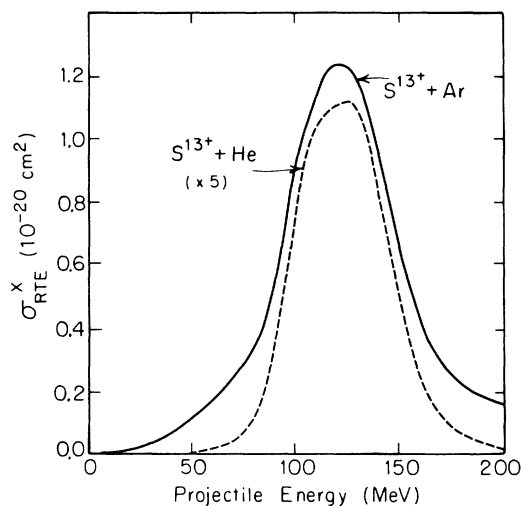


FIG. 2. Total RTE  $K$  x-ray production in  $S^{13+} + Ar$  collisions (solid line) and in  $S^{13+} + He$  collisions (dashed line).

The measurement of RTE cross sections as a function of projectile energy allows one to test calculations of resonance energies and DR cross sections for the projectile and Compton profiles for the target, providing the impulse approximation holds. Then, the shape of the RTE feature reflects the momentum distribution of the target electrons, the position of the cross-section maximum is determined by the resonance energy, and its absolute magnitude is proportional to the DR cross section.

As RTE and REC reflect the momentum distribution of the target electrons in an analogous way, a collisional distortion of the atomic Compton profiles will cause a deviation from the expected shape of both the RTE and REC feature. Thus an experimental study of the same projectile-target combination by both methods would be very interesting.

The experimental observation of RTE can be obscured by a competing process, i.e., excitation due to Coulomb interaction by the target nucleus and electron capture in the same collision. It should be mentioned that interference between RTE and uncorrelated excitation and capture is expected since both processes can populate the same resonance states.

## ACKNOWLEDGMENTS

This work was supported in part by the U. S. Department of Energy, Division of Chemical Sciences. The author is indebted to E. Merzbacher, T. Reeves, and S. Shafroth for valuable discussions.

- <sup>1</sup>J. D. Garcia, R. J. Fortner, and T. M. Kavanagh, *Rev. Mod. Phys.* **45**, 111 (1973).
- <sup>2</sup>J. A. Tanis, S. M. Shafroth, J. E. Willis, M. Clark, J. Swenson, E. N. Strait, and J. R. Mowat, *Phys. Rev. Lett.* **47**, 828 (1981).
- <sup>3</sup>D. Brandt, M. Clark, T. McAbee, P. Peters, S. Shafroth, J. Swenson, and R. Mowat, in *The Twelfth International Conference on the Physics of Electronic and Atomic Collisions, Gatlinburg, 1981*, edited by S. Datz (North-Holland, Amsterdam, 1981).
- <sup>4</sup>J. A. Tanis, E. M. Bernstein, W. G. Graham, M. Clark, S. M. Shafroth, B. M. Johnson, K. Jones, and M. Meron, *Phys. Rev. Lett.* **49**, 1325 (1982).
- <sup>5</sup>H. S. W. Massey and D. R. Bates, *Rep. Prog. Phys.* **9**, 62 (1942).
- <sup>6</sup>M. J. Seaton and P. J. Storey, in *Atomic Processes and Applications*, edited by P. G. Burke and B. L. Moisewitsch (North-Holland, Amsterdam, 1976), Chap. 6.
- <sup>7</sup>D. J. McLaughlin and Y. Hahn, *Phys. Lett.* **88A**, 394 (1982); Y. Hahn (private communication).
- <sup>8</sup>H. W. Schnopper, H. D. Betz, J. P. Delvaille, K. Kalata, A. R. Sohval, K. W. Jones, and H. E. Wegner, *Phys. Rev. Lett.* **29**, 898 (1972).
- <sup>9</sup>M. Kleber and D. H. Jakubassa, *Nucl. Phys.* **A252**, 152 (1975).
- <sup>10</sup>J. S. Briggs and K. Dettmann, *J. Phys. B* **10**, 1113 (1977).
- <sup>11</sup>F. W. Saris, W. F. van der Weg, H. Tawara, and R. Laubert, *Phys. Rev. Lett.* **28**, 717 (1972).
- <sup>12</sup>G. Gerber, R. Morgenstern, and A. Niehaus, *J. Phys. B* **5**, 1393 (1972).
- <sup>13</sup>Yu. S. Gordeev, P. H. Woerlee, H. de Waard, and F. W. Saris, *J. Phys. B* **14**, 513 (1981).
- <sup>14</sup>P. Eisenberger and P. M. Platzmann, *Phys. Rev. A* **2**, 415 (1970).
- <sup>15</sup>F. Biggs, L. B. Mendelsohn, and J. B. Mann, *At. Data Nucl. Data Tables* **16**, 201 (1975).